Technical Sciences
Academy of Romania
www.jesi.astr.ro

Journal of Engineering Sciences and Innovation
Volume 8, Issue 1 / 2023, pp. 1 – 16
http://doi.org/10.56958/jesi.2023.8.1.1

A. Mechanical Engineering

Received ***22 November 2022*** *Accepted* ***24 March 2023***
Received in revised form ***18 January 2023***

The influence of introducing the cohesive zone model in simulating the impact of stratified composites

LARISA TITIRE CHIPER, GEORGE GHIOCEL OJOC, IOANA GABRIELA CHIRACU, LORENA DELEANU*

"Dunarea de Jos" University, Galati, Romania

Abstract. This paper presents a comparison of two models for an impact with a projectile 9 mm FMJ (full metal jacket), having 373 m/s on stratified composites, at meso level. The models contain yarn with the geometry similar to the actual yarns of glass fibers, used in an experimental test. The yarns' orientation is a repeated (0°/90°). The model includs 8 layers of yarns. One model is done including only friction among yarns and between yarn and projectile and the second model introduces both friction and delamination properties (as in the coehesive zone model). The paper reports the differences between the two simulations with the same geometry of the models and the same constitutive material models for yarn and projectile materials, but one with conditioned bonds as in the cohesive zone models. Applying the cohesive zone model (CZM) with zero thickness makes the impact to have a more localized action, reduce bending of the broken yarns. The models are compared to an actual panel made of stratified layers of glass fibers with similar properties of the yarns and the simulation with cohesive zone model gives a closer aspect of the failure as compared to the actual one.

Keywords: stratified composite, simulation, cohesive zone model (CZM).

1. Introduction

Testing campaigns in ballistics are very expensive and time consuming due to materials and technologies involved in producing protective systems, but also due to the number of tests required to assess the system performances [1], [2], [3]. This is why the simulation of such a system behavior helps engineers to restrain the ranges of involved parameters. The big quest is to formulate a model that behaves very close to the actual one. Usually, the steps in producing a protective system

*Correspondence address: lorena.deleanu@ugal.ro

implies documentation, system design, mechanical tests that could help comparing the characteristics with those of existing systems, even if there are not similar to the ballistic impact, designing material and system models and calibrating them according with the preliminary tests, tests on the prototype with actual threats. Based on experimental and simulated data, the design could be improved taking into account different criteria as surface density, personel confort, producing time, price.

This study presents a comparison between two models, one taking into account the friction between the components of the model, target as stratified unidirectional layers and the projectile, 9 mm FMJ (full metal jacket) and the other considering friction and yarns bonded by a cohesive zone with zero thickness, having mechanical characteristics close to the resin matrix ones of the actual composite.

2. The Model

The model has as components the bullet and a panel with 8 layers, each layer including yarns. The projectile is a two-body system, the core made of lead alloy, and the jacket made of copper alloy. The jacket-core connection is a "perfectly bonded" one. The composites is formed with 8 layers of unidirectional yarns made of glass fibers, having the architecture (0°/90°). The yarn section is 0.2 mm x 3 mm.

The scale of the model could be considered as meso because it implies the yarns as a single homogenous isotropic material. The geometry of the model is the same for the two cases. The virtual target has the surface 180 mm x 180 mm (Fig. 1).

There are analyzed two cases, one with only friction among yarns and yarns and projectile and the other one introducing both friction and a cohesive zone betweem each two layers, with zero thickness. For the second case, the connection between each two adiacent yarns is "bonded". This bond could be broken (that is the nodes will detach) if certain values are reached for the tensile stress and the shear stress. These values are given in Tables 3 and 4 and they characterize the resin matrix of this stratified composite.

The option for breaking the node(s) was selected and set with the "Stress Criteria", the failure criterion being defined as:

$$\left(\frac{\sigma_n}{\sigma_n^{limit}}\right)^n + \left(\frac{|\sigma_s|}{\sigma_s^{limit}}\right)^m \geq 1 \quad (1)$$

where σ_n^{limit} is the limit at break for normal stress and σ_s^{limit} is the shear limit at break, and exponents being m=n=2 [4]-[6].

Both cases take into account friction among moving components. the friction coefficient is set as constant, COF = 0.3. Values of COF as found in the literature are ranged from very low (0.05...0.1) to higher (0.3...0.8) [7], [8]. Actually, during the impact, the friction coefficient is not constant and depends on the pair of materials in relative movement and the stress in the normal direction. The broken fibers could increase the abrasive component of friction when the projectile slide against them. Also, the laterally forced plastic deformation of the projectile when it

is arrested change the friction coefficient, including adhesive component, especially with lead alloy.

The projectile model is given in Fig. 1b, also following the dimensions in [9]. The running time was reduced by positioning the projectile as near as possible to the face of the stratified panel (1/4 of a millimeter). Based on the computational resources, the model was run only for a quarter of its geometry, presuming that the two-plane symetry is kept during the impact. A model for the entire system, presented in [10] and [11], but having layers as compact homogenous materials (sheets), proves that there is a certain degree of assymetry in the behavior of the system (reflected in the strain and stress distributions), including projectile position on the target during the penetration.

The yarn was modeled as a body of rectangular cross section, the dimensions being close to the widness of the actual yarn and its thickness is close to that of the fabric layer used in [11].

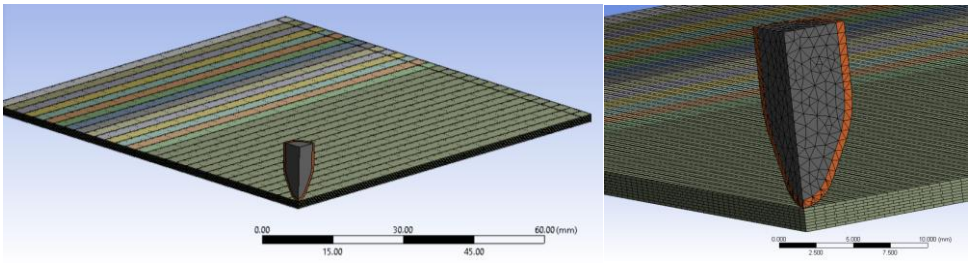

a) general view b) Detail

Fig. 1. The geometry of the model (the quarter of the plate and projectile.

The projectile velocity just before the impact is the initial condition, here v_0 = 375 m/s, as this is also the measured value for the test campaign given in [11]. Each yarn has both their cross ends fixed.

The time interval of the simulation was set for 5×10^{-5} s, the projectile leaving the composite after a total penetration.

The properties of the involved materials in the model are given in Table 1 for the projectile and a yarn. The temperature is set at 22°C for all properties as the model is isothermal. The bilinear model with hardening is often selected to reproduce the mechanical behavior of continuous materials [12]. The yarns are considered continuous bodies with isotropic character, as it is in [13]. There are reports that models with isotropic properties for yarns gave close enough results in order to realistically assess the behavior of the panel [14], [15].

The cohesive zone model (CZM), with zero thickness, is a virtual concept for characterizing the layers' debonding of a stratified composite under loading [16], [17] as the thickness of the matrix between layers (usually fabrics of woven, knited or uniaxial yarns) is very small and may be non-uniform due to the fabrics' architecture. In Explicit Dynamics, the resistance of CZM being nominated as "Bilinear for interface delamination" (Tables 2 and 3) [18], the failure criterion could be "Fracture energies based debonding", for crack opening combined mode.

The difference in the two analyzed cases are discussed based on the equivalent stress distributions on main yarn (the yarn in contact with the projectile during the impact) on each layer, using the function "Path" in Explicit Dynamics. Figure 2a and b presents an exemple for selecting the yarn on layer 4 and Figure 2c gives the von Mises stress distribution along the main yarn on layer 1.

Table 1. Mechanical properties for materials the projectile jacket and core are made of

Property	**Jacket (Copper alloy NL)**	**Core (Lead alloy)**	**Yarns**
Density [kg mm^{-3}]	8.3e-6	1.134e-5	2.54e-6
Specific heat at constant pressure [mJ/(kg °C]	3.85e+5	1.24e+5	
Young modulus [MPa]	1.1e+5	16000	0.13e+5
Poisson coefficient	0.34	0.44	0.25
Biliniar Isotropic Hardening			
Yield Strength [MPa]	280	30	919
Tangent Modulus [MPa]	1150	110	12750
Echivalent plastic strain at break	0.75	0.75	0.03

Table 2. Parameters for modeling in interlaminar delamination

Maximum normal traction stress, MPa	Normal displacement jump at completion of debonding, mm	Maximum tangential traction stress, MPa	Tangential displacement jump at completion of debonding, mm	Ratio
70	5	50	0.1	0.3

Table 3. Parameters for energy at break in delamination

Maximum normal contact stress, MPa	Critical fracture energy for normal separation, J/m^2	Artificial damping coefficient, s
100	3000	0.1

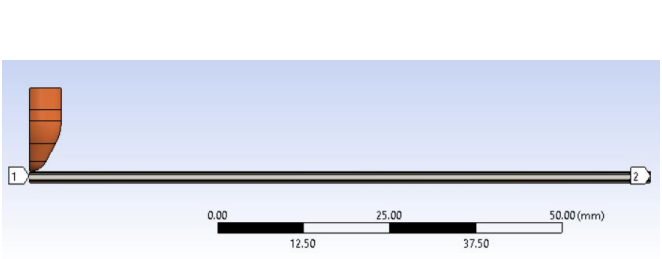

a) Cross section of the model, with a selected path on a layer

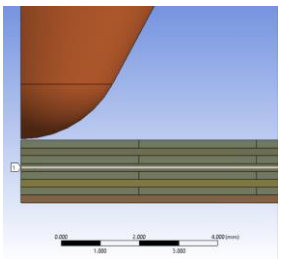

b) Detail of a path selection

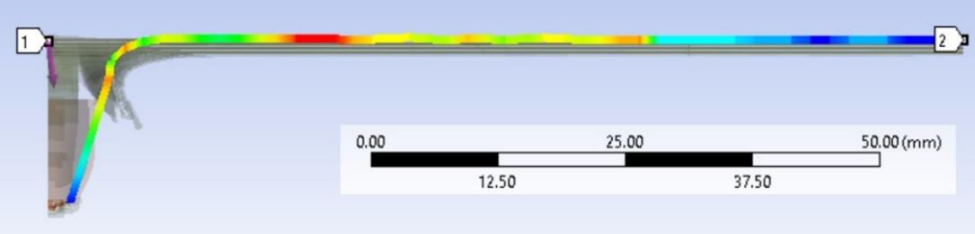

c) Exemple of stress distribution on the yarn on layer 1, at $t=5\times10^{-5}$ s
(red color – high value, blue – lower value)

Fig. 2. Exemple of analyzing the stress distribution olong a yarn (case with CZM)

3. Results and Discussion

The simulation could point out the moment when each yarn is broken by studying the stress evolution on main yarns.
Images extracted from simulation are given in each figure, for both analyzed cases.
Figure 3 presents the first moment of the simulation, $t=2.5\times10^{-6}$ s. The more flexible panel (without introducing CZM) has only one yarn broken on layer 1, but stress distribution is at high values in all the yarn under the projectile. Applying CZM, yarns on layers 1 and 2 are broken but the stress distributions in the following layers is lower (690...350 MPa), enough for not breaking them (yet).
Figure 3 presents the codification of yarns included in the analysis of equivalent stress distribution. Main yarn 1 is the first yarn next to the symmetry plane, under the projectile and main yarn 2 is the yarn next to the main yarn 1. The layers are numbered with 1 for the first layer under the bullet; the uneven layers are considered to have the orientation with 0° and the even layers have the yarn direction perpendicular to the direction of yarns in the unven layers (90°).

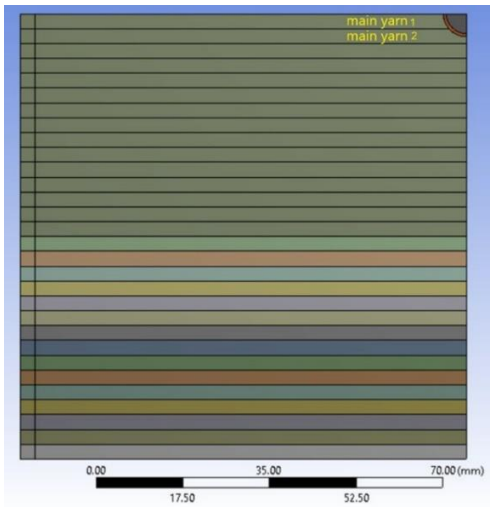

Fig. 3. Codification of the yarns (on each layer), as it is used in plots of stress distribution.

Figure 4 presents the first moment after the impact, considered at 2.5×10^{-6} s. In both cases, the main yarn 1 (0° orientation) on the first layer is broken (von Mises stress drops to zero). This is also pointed out by the graphs of stress distribution along the main yarn 1, presented in Fig. 5.

The values of this stress are similar and the curves have close shapes. But in the case with friction only, the main yarn 1 on layer 2 (with 90° orientation), at this moment, has higher values on the last layer (the 8th one) and the yarn, because, without bonding between yarns and between layers, the bending of the yarns on the last layer is greater.

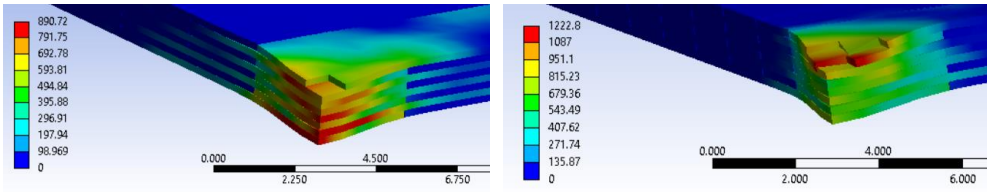

a) With friction only b) With cohesive zone model and friction

Fig. 4. von Mises stress distributions for both cases (in MPa), at moment 2.5×10^{-6} s

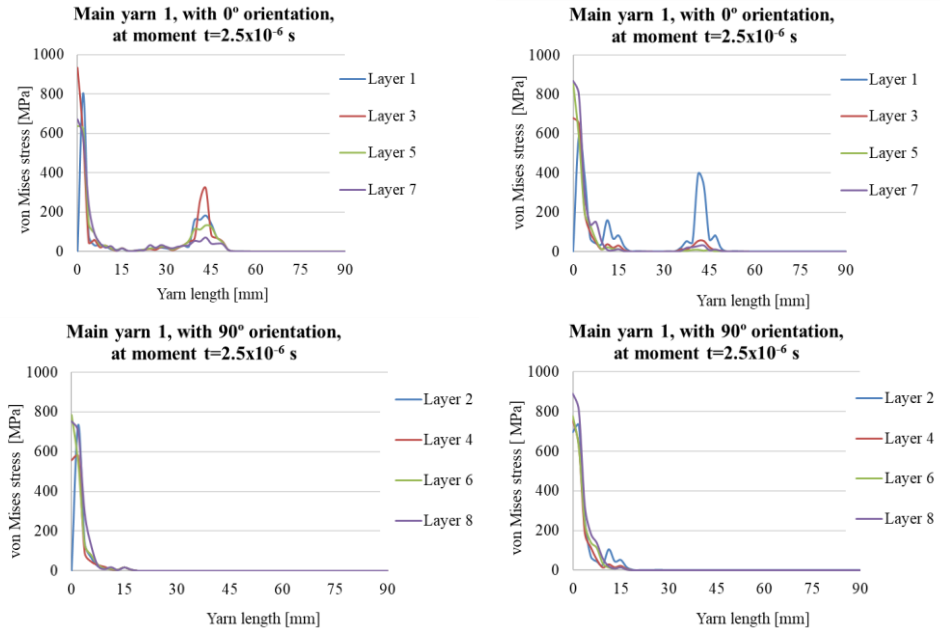

a) Applying CZM and friction b) Applying only friction

Fig. 5. von Mises stress distributions at moment $2.5\text{x}10^{-6}$ s, for each layer

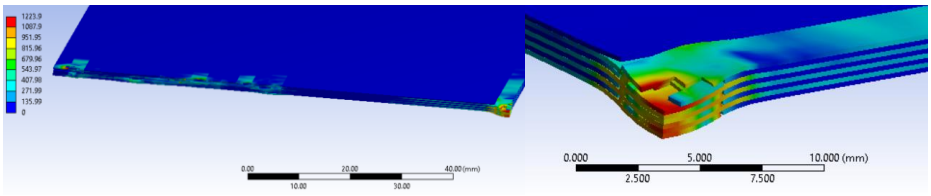

a) With friction only (right – general view, left – detail of the impact zone)

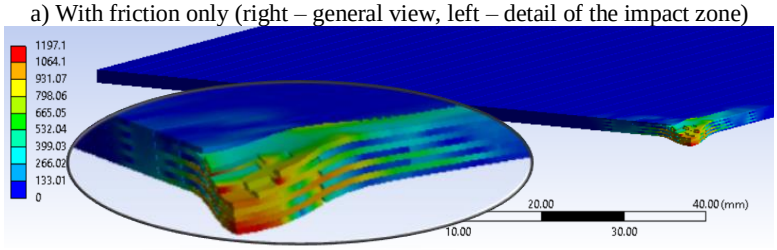

b) with friction and cohesive zone model

Fig. 6. von Mises stress distributions for both cases (in MPa), at moment $t = 5 \times 10^{-6}$ s

Figure 6 presents the von Mises stress distribution for both cases, but at moment $t = 5 \times 10^{-6}$ s. Greater differences appear between the two analyzed cases as compared to the first moment. Yarns arranged without cohesive zone have the value of the equivalent stress high enough 200...500 MPa and stress concentrators are generated near the fixed surfaces of the yarn ends. For the panel with cohesive zone, the stressed volume is smaller but with higher values. The main yarn (the yarn in contact with the projectile) is fragmented under the projectile and ondulated near it. A debonding is visible between the main yarn and the secondary one (the yarn that bears the influence of impact but not in contact with the projectile) is not stressed because it was detached from the yarn bellow it. This is the start of a delamination between layer 1 and the layer 2 on the model with CZM.

Analyzing von Mises stress distributions along the main yarns, at moment $t=5\times10^{-6}$ s, the followings could be noticed (Fig. 7).

- The panel modeled with CZM has already the main yarn 1 broken on layers 1, 2 and 3. These yarns have stress peak near the contact with the projectile due to traction and bending. Yarns on layers 7 and 8 have the highest values for the equivalent stress, around 1100 MPa, meaning it is very probably to be broken because they could have higher displacement (no material behind them, or not too much).
- The panel with yarns without contrainting bonds, but with friction between components, has only the main yarn of layer 1 broken, but all other yarns have high stress values, near the strength limit. The equivalent stress oscilates along all yarns, high value being obtained near the fixed sections for the main yarn on the last layers, 7 and 8.

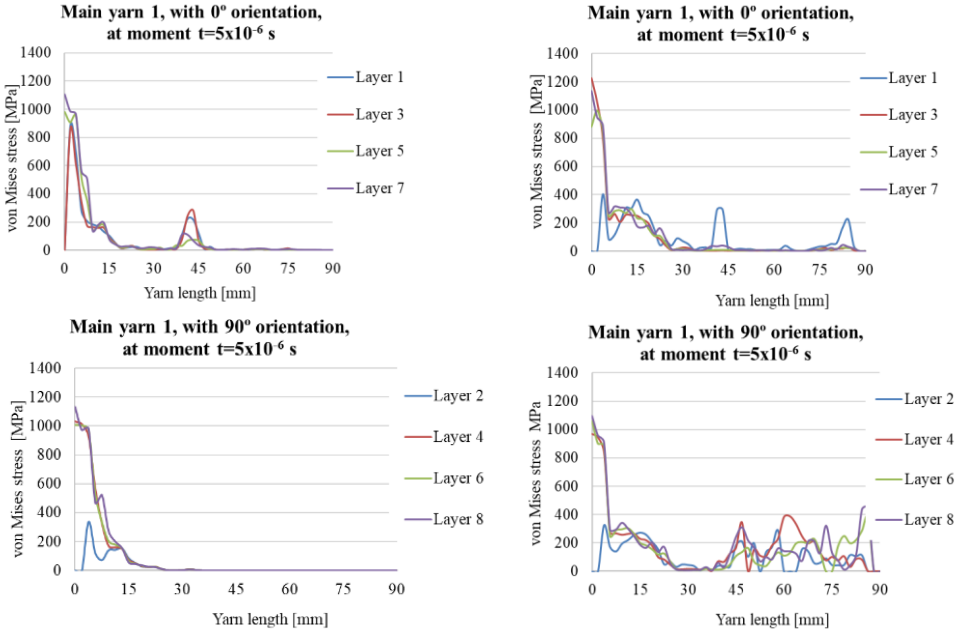

a) with friction and cohesive zone model b) with only friction

Fig. 7. von Mises stress distributions at moment $t=5\times10^{-6}$ s

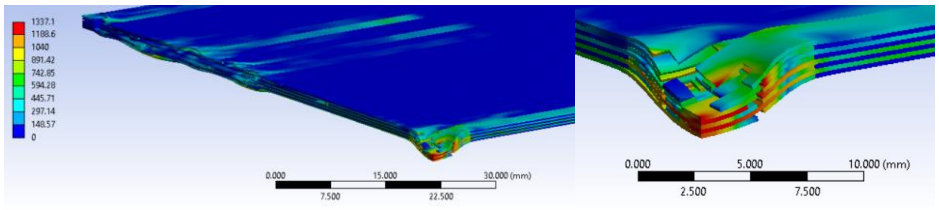

a) With friction

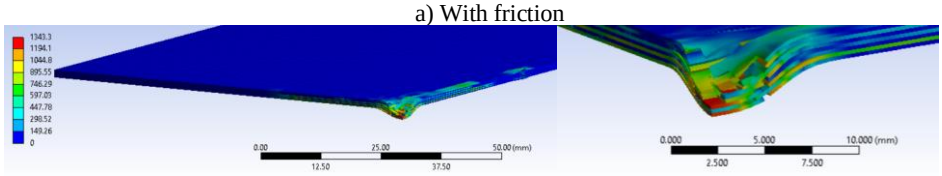

b) with friction and cohesive zone model

Fig. 8. A comparison of von Mises stress distributions between the two analyzed cases (in MPa), at moment $t=1\times10^{-5}$ s

At moment $t=1\times10^{-5}$ s, the impact effects are concentrated arount the direct impact in the panel with CZM, stressed zones are visible also on layer 1, along the main yarn that will cause the debonding of it, without being broken, as it could be seen in Fig. 8. But the model with friction only exhibits larger displacement of the yarns.

Analyzing the stress distributions along the main yarns (Figs. 9 and 10, for two different moments), one may notice that the differences between cases are bigger. The panel modeled with CZM have a smaller zone with high stress (with a radius

of about 45 mm), but for the model with friction only, the yarns are stressed till their fixed ends, the latest layer (the 8th) having high value of the equivalent stress.

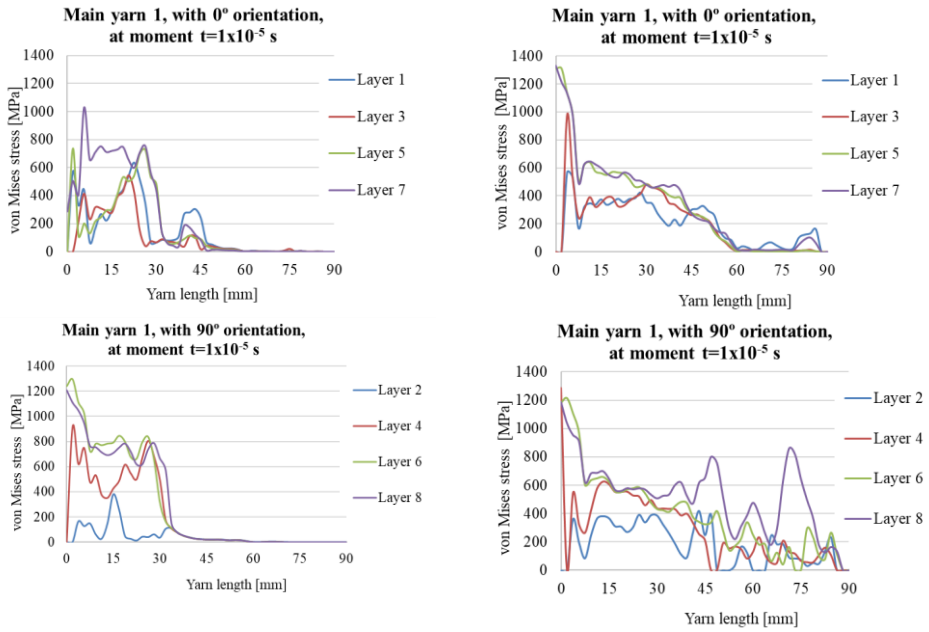

a) with friction and cohesive zone model b) with only friction

Fig. 9. von Mises stress distributions at moment $t = 1 \times 10^{-5}$ s

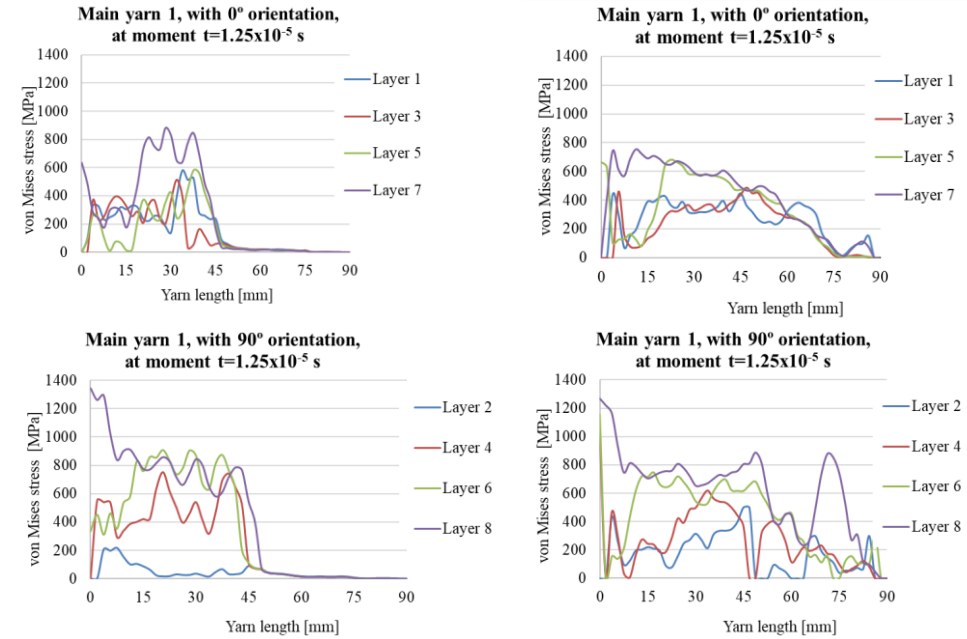

a) with friction and cohesive zone model b) only with friction

Fig. 10. von Mises stress distributions at moment $t=1.25\times10^{-5}$ s

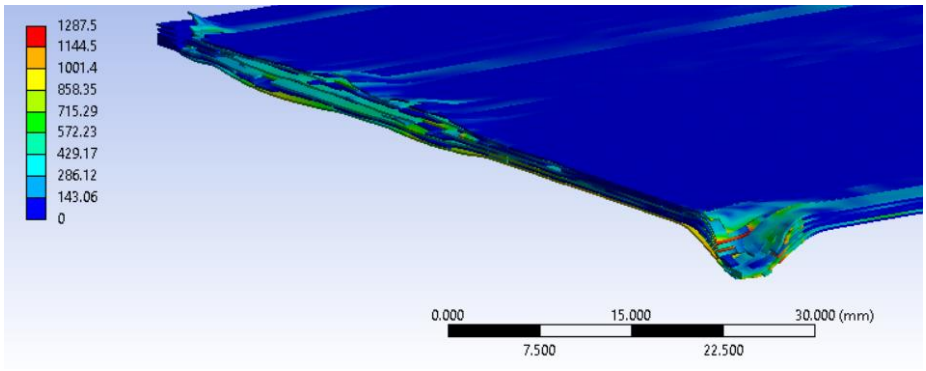

a) with friction only

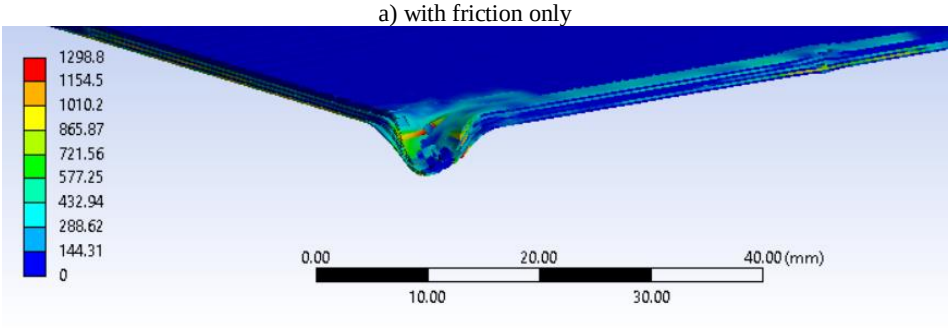

b) with friction and cohesive zone model

Fig. 11. von Mises stress distributions for both cases (in MPa), at moment $t=1.5\times10^{-5}$ s

For the model with CZM (Fig. 10a), yarns on layers 6, 7 and 8 are not broken yet, but have high stress near the projectile due to yarn bending.

The broken yarns have a stress peak positioned at 20...30 mm from the axis of the projectile. Then, the equivalent stress drops to small values (less than 90 MPa). This could reflect the boundary of delamination. Some layers has a zero stress value in or near the axis origine meaning that the yarn was broken in the central zone of the impact, but other yarns have zero stress at a certain distance of the axis meaning that the break is happened in two places, resulting a central fragment, that will form with other similar fragments from other yarns, the so-called cap, more visible at the end of simulation, for both cases. For yarns only arranged one next to the other, the stress is oscillating along the yarns, till their fixed ends (Figs. 10b and 11a).

At 1.5×10^{-5} s, all layers have broken yarns, thus, the penetration is complete for the case applying CZM (Fig. 12a). In the other case, the main yarn on layer 7 is not yet broken (Fig. 12b). This mean that the breakage is more rapid in time for the case with CZM.

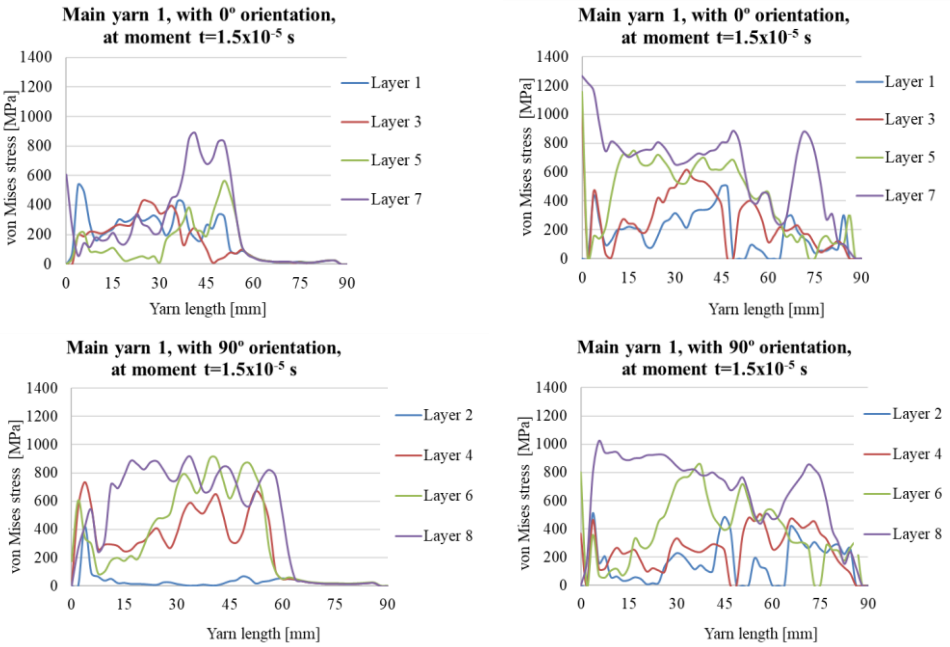

a) with friction and cohesive zone model b) with friction only

Fig. 12. von Mises stress distributions along yarns, at moment $t=1.5\times10^{-5}$ s

To the end of the impact simulation ($t=4\times10^{-5}$ s), there are stress concentrators on the panel with only friction, due to severe bending and local contacts between yarns (Figs. 13a and 14b).

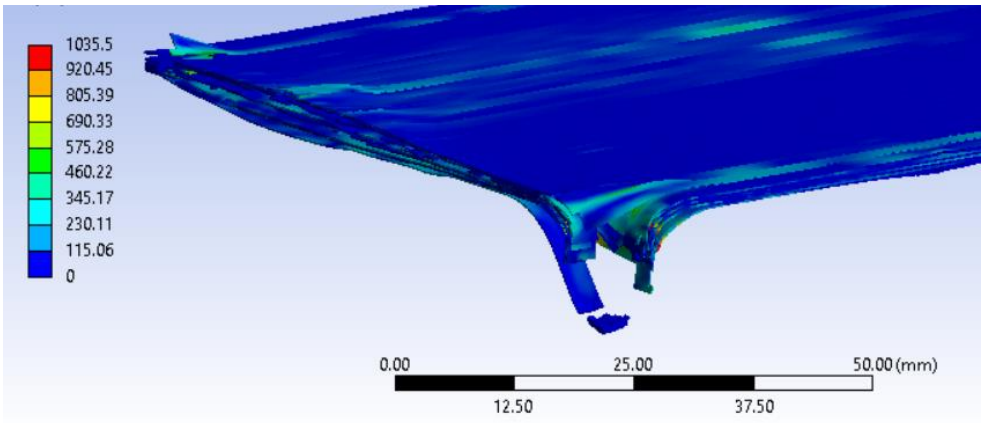

a) with friction only

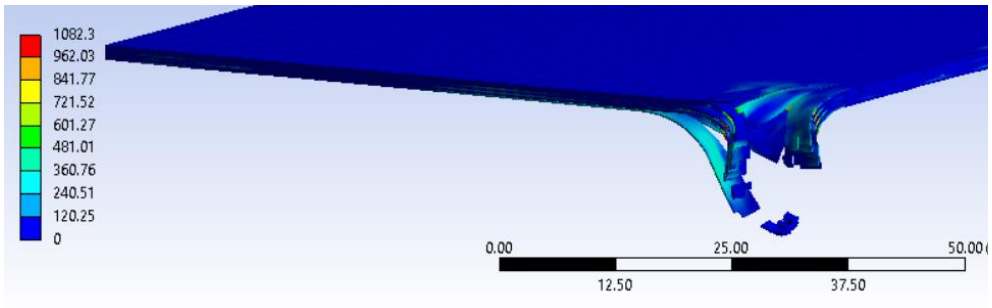

b) with friction and cohesive zone model

Fig. 13. von Mises stress distributions (in MPa), at moment t=4×10^{-5} s

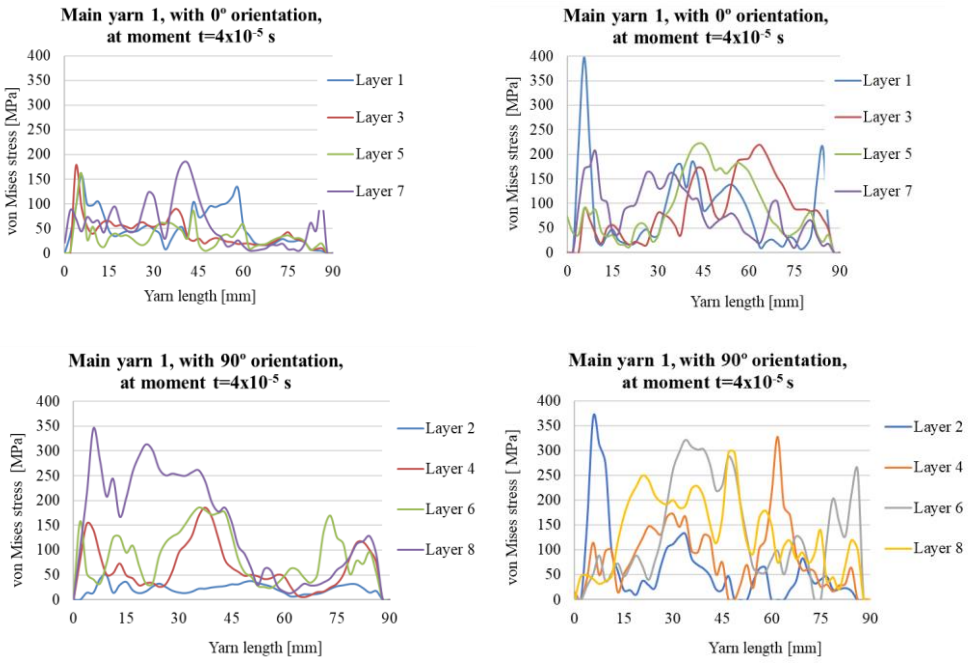

a) with friction and cohesive zone model b) with friction only

Fig. 14. von Mises stress distributions (in MPa) along main yarns, at moment t=4×10^{-5} s

The results of the simulation was qualitatively compared to the actual impact of a 9 mm FMJ projectile on a panel made of stratified unidierctional layers of glass fibers in a resin matrix and the comparison was encouraging the use of the model for evaluating the response of similar composites with different parameters (panel thickness, different projectile as impact velocity, mass and geometry, in a range around the impact velocity in the actual test, v_0 = 375 m/s.

Figure 15 presents a panel made of 8 layers of unidirectional glass fiber fabrics. Each fabric has four sub-layers, with orientation (0°/45°/90°/-45°). On the panel face (the surface first hit by the projectile), the delamination is only visible around

each hole especially for the surface yarns, along the yarn direction. The delaminations resulted around the penetration orifice, after each fire, in the panel, are visible on the panel back (Fig. 14b) and they have a lighter color and an almost circular shape. In a cut section (Fig. 14c), the aspect of the actual orifice is similar to that obtained in the model with CZM.
Information in Table 4 validates that panel modeled with CZM behaves in a similar way to the actual panel.

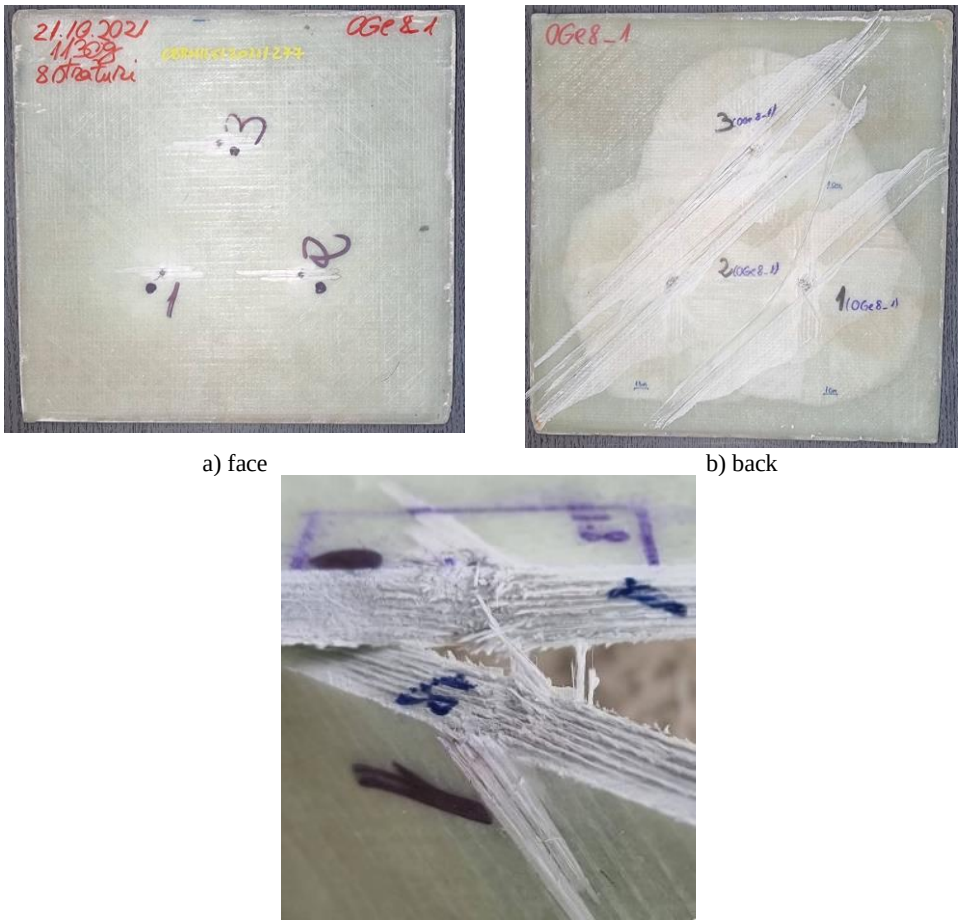

a) face b) back

c) cut section of fire 1

Fig. 15. Actual panel of 8 layers of quadriaxial fabrics, impacted with 9 mm FMJ, at v_0=375 m/s (average).

Table 4. Diameters of the delamination circles on the tested panels (on their back face) and on models

Panel	**Panel thickness (medie)**	**Diameter 1 fire 1**	**Diameter 2 fire 2**	**Diameter 3 focul 3**	**Average diameter**	**Diameter from the model in** [10]	**Diameter from this model with CZM**
	[mm]						
8 layers	6.37	165	165.9	158.09	**162.99**	**117.04**	**120... 124**

4. Conclusions

This study points out the importance of designing protection systems intercorrelating initial design with simulations with simplified models and experimental results.

Figures of equivalent stress distributions at different moments of the imact and images from the run simulations underline that it is important to include in the model the effect of fibers and yarns architecture, their properties and those for their bonding matrix. The athors establish the stages for improving a solution for a protective system: a first design that could be tested in laboratory, a calibrated model based on these first results and that could include one or more parameters to be validated (geometry of the penetration and projectile, qualitative aspect, residual velocity, characteristics determined for particular conditions of the impact as strain rate), a new model (that is validated by laboratory tests or limited tests with actual threat) to use for improving the initial solution or to determine the range of threats that the system could safely face. The last tests should be done on actual system, with actual threats, for a number of tries as required by standards and experience of the users.

This study proposed a comparison between two models of a panel made of 8 layers, ecah one having unidirectional yarns (with the thickness of the actual fabric layers used in actual tests): one presumes that friction exists among yarns and yarns and projectile and it is an ideal case as in reality, yarns have to be kept together in a matrix and the other one that includes yarns bonded face-to-face by a coehesive zone (with zero thickness), but having the mechanical properties of a resin recommended as matrix for such a composite. Friction is also included in the second case. The threat and the initial condition (v_0=375 m/s) are the same for both cases and the results are interpretated taking into consideratin the delamination and the penetration aspect characterizing the model and actual tests.

The presence of the cohesive zone among yarns reduces the delamination and the tendency of breaking yarns near the fixed ends (due to excessive bending) and the failure aspect of first and last layers is realistic as compared to the actual panel of the same thickness. Even if the model was run at meso scale (with yarns as compact bodies) and the materials' models are considered bilinear and isotropic, the behavior of the model was realistic.

Acknowledgement

The authors would like to thank to their colleagues from INAS Craiova, as they offer effective recommendations in order to fulfill this study.

References

[1] Bhatnagar A., *Lightweight Ballistic Composites* (2nd edition), Elsevier, Amsterdam, 2016.
[2] *** Ballistic Resistant Protective Materials, NIJ Standard 0108.01
[3] Abtew A. M., Boussu F., Bruniaux P., *Dynamic impact protective body armour: A comprehensive appraisal on panel engineering design and its prospective materials*, Defence Technology, **17**, 2021, p. 2027-2049
[4] Jinescu V. V., A*pplication in Mechanical Engineering of Principle of Critical Energy*, Lambert Academic Publishing, Saarbrücken, 2015.
[5] Jinescu V. V., Nicolof V. I., Chelu A., Manea S. E., *Calculation of the local critical state taking into account the deterioration and the residual stresses*, Journal of Engineering Sciences and Inovation, **2,** 3, 2017, p. 9-21.
[6] Sridharan S., Li Y., Competing cohesive layer models for prediction of delamination growth, p. 369, 2008, in Delamination behaviour of composites, editor Sridharan S., Woodhead Publishing LTD, Cambridge, UK
[7] Ingle, S., Yerramalli, C. S., Guh,a A., Mishra, S. *Effect of material properties on ballistic energy absorption of woven fabrics subjected to different levels of inter-yarn friction.* Composite Structures, **266**, 2021,113824. doi: 10.1016/j.compstruct.2021.113824
[8] Meyer, C. S., O'Brien, D. J., (Gama) Haque, B. Z., Gillespie, Jr. J. W. *Mesoscale modeling of ballistic impact experiments on a single layer of plain weave composite*. Composites Part B, **235**, 2022, 109753
https://doi.org/10.1016/j.compositesb.2022.109753
[9] Wiśniewski A., Gmitrzuk M., V*alidation of numerical model of the Twaron CT709 ballistic fabric*. Proceedings of 27th International Symposium on Ballistics, BALLISTICS 2013, **2**, 2013, 1535-1544.
[10] Pirvu C., *Contribution on Experimental and Numerical Study of Ballistic Protection Packages Made of Aramid Fabrics* (in Romanian), PhD, "Dunarea de Jos" University, Galati, Romania
[11] Ojoc G. G., *A Theoretical and Experimental Study of Ballistic Protection Packages Made of Glass Fibers*, PhD, "Dunarea de Jos" University, Galati, Romania, 2022
[12] Năstăsescu V., Ştefan A., Lupoiu C., *Analiza neliniară prin metoda elementelor finite. Fundamente teoretice şi aplicaţii*, Academia Tehnică Militară, Bucharest, 2001.
[13] Wei Q., Yang D., Gu B., Sun B., *Numerical analysis of strain rate effect on ballistic impact response of multilayer three dimensional angle-interlock woven fabric*, International Journal of Damage Mechanics, 0(0) 1–22, 2021, DOI: 10.1177/1056789520983598
[14] Wang, Y., Chen, X., Young, R., Kinloch, I., & Wells, G. *A numerical study of ply orientation on ballistic impact resistance of multi-ply fabric panels*, Composites Part B: Engineering, **68**, 2015, 259–265. doi:10.1016/j.compositesb.2014.08.049
[15] Yang, Y., Chen, X. *Influence of fabric architecture on energy absorption efficiency of soft armour panel under ballistic impact*. Composite Structures, **224,** 2019, 111015. doi:10.1016/j.compstruct.2019.111015
[16] Joki, R. K., Grytten, F., Hayman, B., Sørensen, B. F., *Determination of a cohesive law for delamination modelling - Accounting for variation in crack opening and stress state across the test specimen width.* Composites Science and Technology, **128**, 2016, 49-57. doi: 10.1016/j.compscitech.2016.01.026

[17] Chowdhury, U., Wu, X.-F. *Cohesive zone modeling of the elastoplastic and failure behavior of polymer nanoclay composites*, Journal of Composites Science, **5**, 2021, p. 131, https://doi.org/10.3390/jcs5050131
[18] ***ANSYS Explicit Dynamics Analysis Guide, 2021, ANSYS, Inc., USA